THE GEOMETRY OF PERIPHERAL MYELIN SHEATHS DURING THEIR FORMATION AND GROWTH IN RAT SCIATIC NERVES

HENRY DEF. WEBSTER

From the Laboratory of Neuropathology and Neuroanatomical Sciences, National Institute of Neurological Diseases and Stroke, National Institutes of Health, Bethesda, Maryland 20014

ABSTRACT

In rat sciatic nerves, a small bundle of fibers was identified in which myelin sheaths were absent at birth, appeared within 3 days, and grew rapidly for 2 wk. During this interval, nerves were removed from littermates and were sectioned serially in the transverse plane. Alternating sets of thin and thick sections were used to prepare electron micrograph montages in which single myelinating axons could be identified and traced distally. During the formation of the first spiral turn, the mesaxon's length and configuration varied when it was studied at different levels in the same Schwann cell. The position of the mesaxon's termination shifted while its origin, at the Schwann cell surface, remained relatively constant. Along myelin internodes composed of two to six spiral turns, there were many variations in the number of lamellae and their contour. Near the mesaxon's origin, longitudinal strips of cytoplasm separated the myelin layers. Thicker sheaths were larger in circumference, more circular in transverse sections, and more uniform at different levels. Irregularities were confined to the paranodal region, and separation of lamellae by cytoplasm occurred at Schmidt-Lantermann clefts. Approximate dimensions of the bundle, its largest fibers, and their myelin sheaths were measured and calculated. The myelin membrane's transverse length and area increased exponentially with time; the growth rate increased rapidly during the formation of the first four to six spiral layers and remained relatively constant during the subsequent enlargement of the compact sheath.

INTRODUCTION

In 1954, the observations and hypothesis of Geren clearly established the basic morphological parameters of myelin formation in peripheral nerves (1). Additional evidence to support her hypothesis was published during the next few years (2–4). The mesaxon, which is continuous with the Schwann cell surface membrane, elongates to form a spiral around the axon. Further growth and apposition of the spiral layers occur as the myelin sheath matures. Since then, these observations have been confirmed and extended by many investigators (see, for example, references 5–20). In general, they have agreed that the Schwann cell, or part of its surface, moves around the axon during growth of the myelin spiral (1, 7, 8, 13). Two other observations that are not readily explained by any simple rotation hypothesis have also been discussed. The contour of the myelin spiral is not uniform along the internode; complex variations occur (21–23). Secondly, after the compact sheath is formed, its internal circumference increases to accommodate the growing axon (3, 7,

12, 23, 13). Also, a review of the literature has revealed that our morphological concepts of myelination in nerves have been based mainly on the electron microscope appearance of nerves that have been sectioned transversely and studied at a single level.

In spite of its importance, the three-dimensional form of myelinating axons and their Schwann cells has been investigated only in a few fibers over relatively short distances (7). Recently, the availability of decontamination devices for electron microscopes has made it easier to examine much larger areas in thin sections. Also, when fixation of tissue in permanganate is preceded by immersion in aldehyde (24), better over-all preservation can be achieved than with the use of permanganate alone. Therefore, it seemed worthwhile to plan an investigation of serially sectioned nerves that would define more completely the geometry and dimensions of the myelin spiral during its formation and growth in the Schwann cell.

In this study, a small bundle of fibers in rat sciatic nerves was identified in which myelination occurred during the 2 wk after birth. At age 1 wk, when all stages of this process were widely represented, 50 axons and their satellite Schwann cells were traced and compared in a series of electron micrograph montages. Approximate dimensions of the bundle, its largest fibers, and their myelin sheaths are also included in this report which has been summarized previously (25).

METHODS

Tissue Preparation

At age 1, 3, 7, and 16 days, Sprague-Dawley rats from two litters were anesthetized with an intraperitoneal injection of 0.1–0.8 ml of 4% chloral hydrate. The right sciatic nerves were carefully exposed and fixed *in situ* for 10 min with a 2% glutaraldehyde (Union Carbide Co., New York, biological grade) solution containing 0.33% acrolein, 0.5% calcium chloride, and 0.07 M sodium cacodylate (pH 7.1–7.3). When the nerves were removed, a small muscular branch that emerged near the mid-thigh level was included in the resection to serve as a landmark. These sciatic nerves were immersed in the above solution for 20 min at 4°C and then transferred to 6% aqueous potassium permanganate (pH-7.5) for 1 hr. The temperature of this solution was 4°C, and it was filtered just before use. Several brief rinses in 0.2 M chilled sodium cacodylate buffer were used for removing excess permanganate from the nerves before dehydration. Different solutions were employed to fix the left sciatic nerves which were processed according to the above procedure along with those from the opposite side. The composition of the initial fixative (pH 7.4) was 2% glutaraldehyde, 0.33% acrolein, 0.002% calcium chloride, and 0.05 M Sorenson's phosphate buffer. The second solution (pH 7.4) contained 2% osmium tetroxide, 0.002% calcium chloride, 0.05 M Sorenson's phosphate buffer, and 3% sucrose. Also, these nerves were not rinsed in buffer before being transferred to dilute alcohol.

All of the nerves were dehydrated in ethanol: 15 min each in 25, 35, 50, 70, and 95% ethanol at 4°C, then two changes of 30 min each in absolute ethanol at room temperature. After 5 min of immersion in propylene oxide, the nerves were transferred to a 1:1 combination of Epon mixture (Fisher Scientific Co., Pittsburgh, Pa., 100 ml–48 ml Epon, 21 ml dodecenylsuccinic anhydride [DDSA], 31 ml nadic methyl anhydride [NMA]) and propylene oxide (26). The uncovered weighing bottles were agitated overnight (27), and the propylene oxide evaporated gradually. The following day, each nerve was transected just proximal to the muscular branch described above. Both the proximal and distal pieces were oriented in molds (28) so that the mid-sciatic end of each one could be sectioned transversely. Fresh Epon mixture, with 1.5 ml of 2,4,6,-tri(dimethylaminomethyl) phenol (DMP) added per 100 ml, was used to fill the molds which were then heated to 40°C for 7 hr and 60°C for 16 hr.

Electron Micrograph Montages

2-μ sections of both pieces were studied by phase microscopy so as to establish the level of transection. When necessary, more sections of the appropriate block from each nerve were mounted serially and compared until the fascicular topography in the transverse sections from all the nerves in the series was similar. At this level, the posterior tibial divisions were oval or circular and their perineuria were fused or immediately adjacent to each other. (More proximally, a perineurial septum was located between the two divisions that formed a single circular bundle; distally, the two divisions were separated by epineurium.) Along the edge of the posterior tibial fascicle at the desired level, there was a small bundle of fibers that usually extended from the region where the perineuria fused along a 90° arc. Centrally, a row of fibroblasts separated this thin segment from the remainder of the posterior tibial fascicle. In four littermates, age 1, 3, 7, and 16 days, the appearance of the right and left sciatic nerve sections also corresponded closely. Without trimming the blocks further, thin sections of these four right sciatic nerves were cut and mounted on Formvar-coated grids with a 1 × 2 mm central opening. They were stained with lead citrate (29) and examined in a Philips EM 300

electron microscope equipped with a decontamination device. The marginal bundle described above was easily located because the whole sciatic nerve was included in thin sections that were supported only by a Formvar film. For the nerves removed at 1, 3, and 7 days of age, overlapping areas of the entire marginal bundle were photographed at an electron optical magnification of 5000. 8 × 10 inch micrographs, at a final magnification of 12,500, were mounted together to make each montage. In the montage of the 1-day old nerve, there were no compact myelin spirals; at 3 days, less than 2% of the axons in this bundle were surrounded by a compact sheath. However, in the montage of the 7 day old nerve, all stages of myelin formation were widely represented. Finally, a survey of the same bundle in the 16 day old nerve revealed that almost all of the myelin sheaths had 10–40 compact lamellae; very few axons were surrounded by spirals consisting of only a few turns.

Therefore, the 7 day old nerve seemed best suited for further study. 30 transverse sections, 2 μ in thickness, were mounted serially before thin sections were cut again for another montage. This procedure was repeated until the same group of fibers was present in a distally progressing sequence of 16 montages. The first ten were separated by about 60 μ and the last seven were approximately 8 μ apart.

In the tenth montage, 50 axons were numbered that varied in diameter and were surrounded by Schwann cell mesaxons, loose spirals, or compact myelin sheaths. These axons were identified in each distal montage and in the intervening, serially mounted sections that were 2 μ thick. The following data were recorded: the axon diameter (measured in mm on each montage); the transverse levels of its Ranvier nodes and Schwann cell nuclei; the mesaxon origin at the surface membrane and its termination adjacent to the axon (for each, clock numerals 1–12, using the same reference points at distal levels for orientation); the spiral direction from origin to termination (clockwise, anticlockwise, reversals, variations); the number of spiral turns or myelin lamellae; in compact myelin sheaths, the incidence and extent of contour variations (loops, lamellar ovoids, incisures, as well as other regions where cytoplasm was located between compact lamellae). Representative areas that included the same fibers at each level were traced on 4 × 5 inch glass slides and mounted on racks as partial reconstructions. Electron micrographs, exposed at higher magnification, were used to study membrane relationships in greater detail.

Measurements and Calculations

At each age interval, both the serially mounted 2-μ sections and the montages were used to obtain some approximate dimensional changes in the marginal bundle and its largest fibers (Tables I and II). This bundle was identified also in sections from an adult sciatic nerve that was included for comparison. The approximate area of this bundle was calculated from measurements of the arc (θ, in degrees) forming its surface margin and the radius of the posterior tibial fascicle according to the formula for the area of a circle's segment:

$$A = \frac{\Pi r^2 \theta}{360} - \frac{r^2 \sin \theta}{2}.$$

Then, the internodal region of five of the bundle's largest fibers was identified at each interval in electron micrographs at magnifications of 9000–17,000. Each Schwann cell was measured, and its dimensions were calculated separately. The diameters (if noncircular, the average of a mutally perpendicular maximum and minimum) of the axonal and endoneurial surface were measured; their sum, multiplied by Π provided the surface membrane circumference. The length of the myelin membrane in the transverse plane was estimated in the following manner. It is apparent that the mesaxon is a pair of membranes in continuity with a unit membrane at the endoneurial and axonal surfaces. Contour irregularities were neglected, and the spiral myelin membrane was considered as a set of 2N concentric circles where N was the number of turns in the mesaxon spiral or the number of dense lines in the compact sheath. The product of M, the measured diameter to points midway between the inner and outer spiral layers, and 2 Π N was the approximate length of myelin membrane in the transverse plane. For the 7-,16, and 75-day old nerves, the surface and myelin membrane areas were calculated for each Schwann cell after its length was obtained from the locations of its nodal ends and nucleus in the serially mounted sections that were 2 μ thick. Appropriate series of montages and serial sections were not available for measuring the Schwann cell lengths in the 1 and 3 day nerves. Their membrane areas were calculated by using the mean lengths of comparable Schwann cells in the 7 day nerve (Table II, 53 and 68 μ).

The above procedure was also used to obtain all the other dimensions that are included in Table II.

RESULTS

The phase microscope appearance of the sciatic marginal bundle from 1-, 3-, 7-, and 16-day old rat littermates is illustrated at the same magnification in Fig. 1. Its approximate area and some dimensions of its largest fibers are given in Table I.

On the day of birth (Fig. 1 *a*), no compact myelin sheaths were present and the area of the

TABLE I

Approximate Dimensional Changes with Age in Rats' Marginal Sciatic Nerve Bundle and Its Largest Fibers

Age	Marginal bundle	Mean Values For Five of Bundle's Largest Fibers						
Calculated	Calculated area	Axon diameter	Myelin spiral number of turns	Schwann cell surface membrane circumference	Myelin membrane transverse length of spiral	Schwann cell longitudinal length	Schwann cell surface membrane area	Schwann cell myelin membrane area
Days	μ^2	$\mu \pm$ SE	*Range*	$\mu \pm$ SE	$\mu \pm$ SE	$\mu \pm$ SE	$\mu^2 \pm$ SE	$\mu^2 \pm$ SE
1	2100	1.2 ± .1	½–1	11.4 ± .5	7.4 ± 1.2	—	6×10^{2}*	4×10^{2}*
3	2500	1.4 ± .1	2¾–4	13.8 ± .6	$(4.4 \pm .6) \times 10^{1}$	—	9.4×10^{2}*	3×10^{3}*
7	7500	1.6 ± .1	17–28	13.7 ± .6	$(2.8 \pm .3) \times 10^{2}$	100 ± 20	$(1.5 \pm .2) \times 10^{2}$	$(3 \pm .3) \times 10^{4}$
16	12,000	2.2 ± .1	35–53	23 ± .8	$(1.0 \pm .1) \times 10^{3}$	220 ± 15	$(5.0 \pm .5) \times 10^{3}$	$(2.0 \pm .2) \times 10^{5}$
75 (Adult)	21,000	5.9 ± .1	72–94	50 ± 2	$(4.0 \pm .2) \times 10^{3}$	650 ± 90	$(3.0 \pm .2) \times 10^{4}$	$(2.6 \pm .2) \times 10^{6}$

* Mean lengths for Schwann cells from the 7 day nerve were used to calculate these values. See Table II and Text.

TABLE II

Mean Dimensions for Groups of Five Fibers in Marginal Bundle from a 7 Day Old Rat Sciatic Nerve

Myelin spiral No. of turns	Axon diameter	Schwann cell surface membrane circumference	Myelin membrane transverse length of spiral	Schwann cell longitudinal length	Schwann cell surface membrane area	Schwann cell myelin membrane area
Range	$\mu \pm$ SE	$\mu \pm$ SE	$\mu \pm$ SE	$\mu \pm$ SE	$\mu^2 \pm$ SE	$\mu^2 \pm$ SE
½ – ⅞	1.2 ± 0.1	9.9 ± 0.5	5.6 ± 1.1	53 ± 4*	$(5.2 \pm 0.5) \times 10^{2}$	$(2.8 \pm 0.2) \times 10^{2}$
3–4	1.2 ± 0.1	11.2 ± 0.9	$(3.0 \pm 0.3) \times 10^{1}$	68 ± 7.5*	$(7.6 + 1.3) \times 10^{2}$	$(1.9 \pm 0.1) \times 10^{3}$
4–6¼	1.5 ± 0.1	11.9 ± 1.1	$(6.0 \pm 0.5) \times 10^{1}$	60 ± 5.5	$(7.7 \pm 1.5) \times 10^{2}$	$(3.7 \pm 0.8) \times 10^{3}$
17–28	1.6 ± 0.1	13.7 ± 0.6	$(2.8 \pm 0.3) \times 10^{2}$	100 ± 20	$(1.5 \pm 0.2) \times 10^{2}$	$(3.0 \pm 0.3) \times 10^{4}$

* These Schwann cell lengths were used to calculate the areas for the one and three day intervals in Table I. See text.

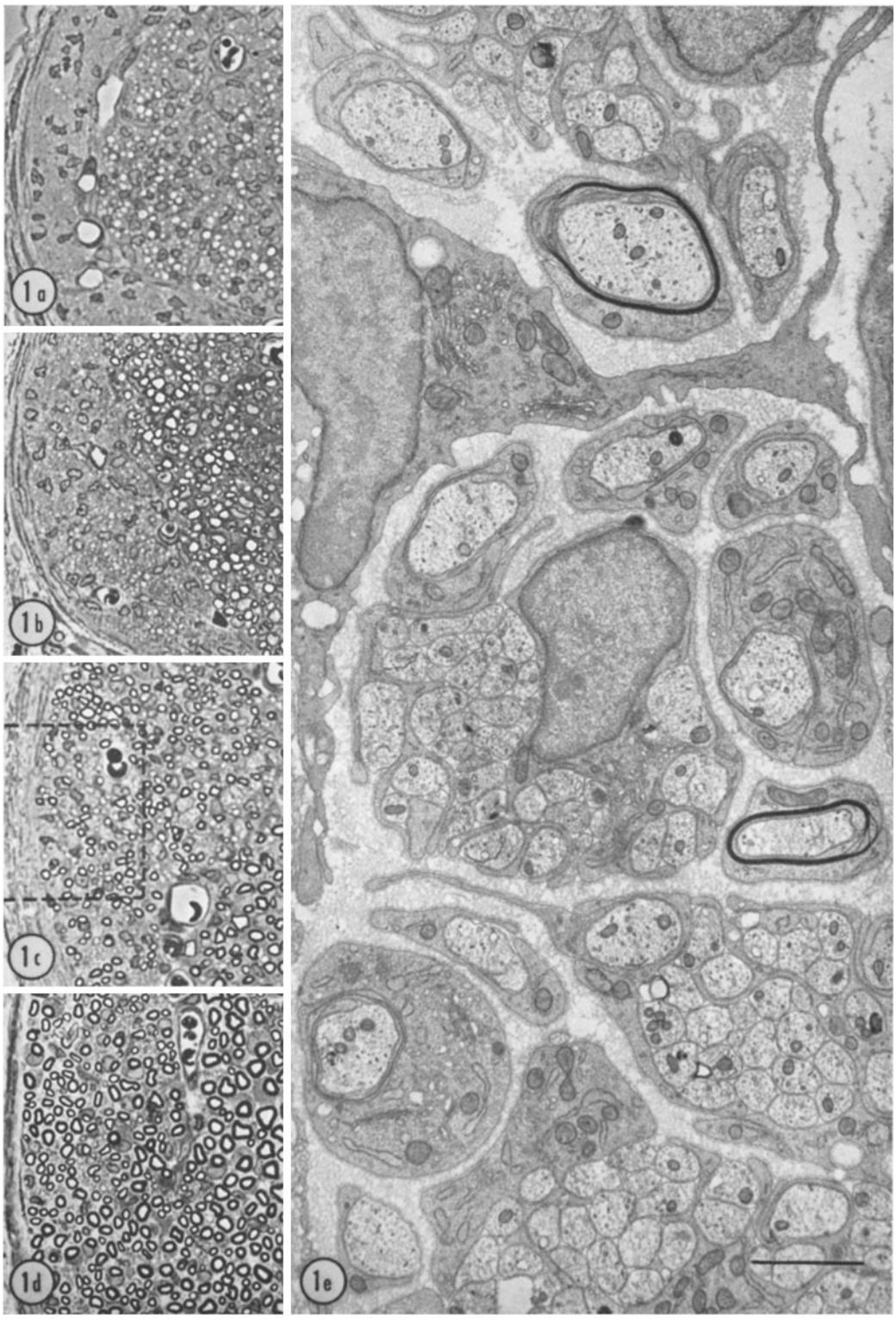

FIGURE 1 Transverse sections at the same magnification (*a–d*) of the marginal bundle in rat sciatic nerves. The perineurium of the posterior tibial fascicle is to the left. At birth (Fig. 1 *a*), there are no compact sheaths, and at age 3 days (Fig. 1 *b*) there is only one. At age 7 days (Fig. 1 *c*), many are apparent; the area included in the montages is outlined. The myelin sheaths are more numerous and larger at age 16 days (Fig. 1 *d*). × 500. 11 of the 50 fibers traced in the montages are shown in Fig. 1 *e*. Five surround the central Schwann cell; to the right of its nucleus, there is a segregated fiber with a short mesaxon. × 17,000.

bundle was about 2500 μ^2. Mesaxons with ½–1 spiral turn were identified around the largest axons which measured 1.2 μ in diameter. At age 3 days, the area of the marginal bundle was 1.2 times its size at birth (Fig. 1 *b*). The proportion of axons with mesaxon spirals had increased, and the largest had 2¾–4 turns. Only one compact myelin sheath was present. At age 7 days, the bundle's area was much greater. Also, there were many compact myelin sheaths (Fig. 1 *c*). Some of the largest had 17–28 spiral turns, were 70–120 μ long, and surrounded axons with diameters of approximately 1.6 μ. An arbitrary area, corresponding to that outlined in Fig. 1 *c*, was included in the electron micrograph montages used for identifying and tracing the 50 fibers described below. Some of them are illustrated at low magnification in Fig. 1 *e*. Both at age 16 days (Fig. 1 *d*) and in the adult (not illustrated), the number of compact myelin sheaths, their size and the area of the entire bundle were larger. Also, it is clear from the data in Table I that the dimensions of this bundle and its largest fibers increased with age at different rates. In the transverse plane, the increases in the diameters of axons and the circumferences of their Schwann cell surface membranes were similar to the radial growth of the posterior tibial fascicle. By age 16 days, these dimensions were about twice their size at birth, and they doubled again by adulthood. However, the transverse lengths of the myelin membrane in the same Schwann cells increased much more rapidly. From birth to age 16 days, there was more than a 100-fold change. The growth rate was greatest during the 1st wk and decreased with time; the adult value was about four times larger than the value for the 16 day myelin membrane. In the longitudinal plane, measurements of the Schwann cells' length in the 1- and 3-day old nerves were not available. Its subsequent increases were slightly greater than those for the first two transverse dimensions; these differences are reflected in the membrane areas and their growth rates.

When the 50 axons from the 7-day nerve were ranked according to the maximum number of mesaxon or myelin spiral turns around each one, the following distribution was obtained: There were 12 axons in the first group. In each of their Schwann cells, the mesaxon spiral was more than one-quarter but less than one turn at all levels. The next group of 13 axons had myelin sheaths that formed a transition sequence from a single mesaxon loop to a compact lameller spiral with six turns. In the last group, the appearance of the myelin sheaths was similar to that observed in adult rats; Schmidt-Lantermann clefts were the only interruption in their compact spiral structure. 16 axons had sheaths with 7–12 turns and the last nine had 13–28 turns. Each of these three groups is described separately; fiber dimensions are included in Table II.

Formation of the First Spiral Turn

When the data for the 12 axons, their Schwann cells, and mesaxons were compared, the variability in all the dimensional and descriptive parameters was the most consistent and obvious feature. In this group, the axons measured 0.7–1.0 μ in diameter. At a single level, a few were embedded separately in the perinuclear region of Schwann cells that surrounded other smaller unmyelinated fibers (Fig. 1 *e*). These were the smallest mesaxons (¼–½ spiral turn, traced longitudinally for less than 8 μ) and were considered to represent the onset of myelin formation. In proximal or distal montages, each of these axons was enveloped by its own Schwann cell. The neighboring satellite cells were not separated by basal laminas or endoneurial collagen, and thus appeared to belong to the same family (Figs. 1 *e*, 2–4). This type of surface relationship was identified for varying longitudinal distances in all of this group's Schwann cells. Occasionally, it was possible to identify the nuclei of the neighboring cells in successive thin sections at the same level (Figs. 2–4). In a few instances, the Schwann cells surrounding different groups of small unmyelinated fibers were the surface neighbors of the same Schwann cell. In the example illustrated in Fig. 7, three small axons that lie on the surface of the linking cell (Fig. 7 *c*) can also be traced from a proximal Schwann cell at the lower left in Fig. 7 *b* to a distal one to the right of center in Fig. 7 *d*.

The mesaxons in this group's Schwann cells had ¼–1 turn, were 25–64 μ long, and were not uniform spirals. Generally, their origins at the Schwann cell surface were in the same quadrant at all levels. Shifts of 90–180° were most frequent near the nucleus especially if it was helical (Fig. 7), instead of ellipsoid in shape or if it was not located midway between the proximal and distal ends. The number of turns was usually greater in the paranuclear region than at either nodal end. However, no orderly progression was observed, and differ-

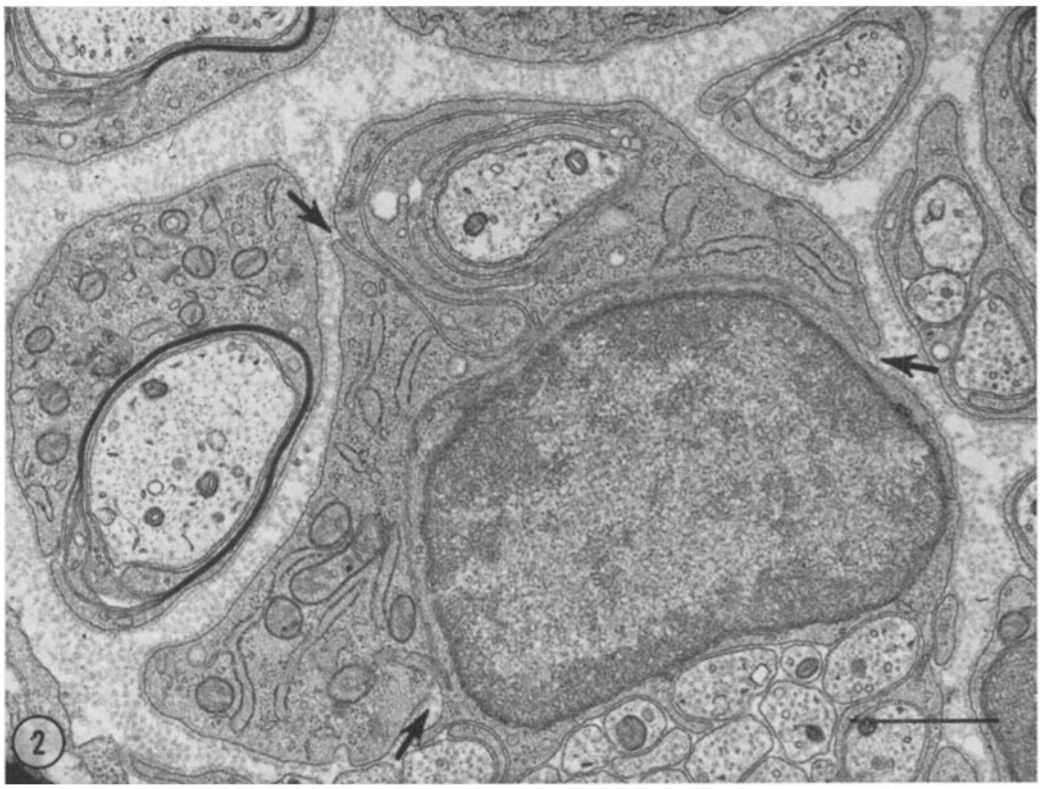

FIGURES 2–4 Two adjacent Schwann cells and their nuclei are shown in the same set of thin sections. In Fig. 2, their surface membranes (lower arrows) are above the nucleus of the lower Schwann cell which surrounds many unmyelinated axons. Both nuclei and the cell membranes between them (lower arrows) are shown in Fig. 3. In Fig. 4, the surface membranes are below the nucleus of the upper Schwann cell. The origin of this cell's mesaxon (upper arrow) is in the same quadrant in all of the figures although its contour varies. × 20,000.

ences between levels were proportional to the quantity of adjacent cytoplasm. The mesaxons' direction and contour were highly variable in different thin sections at the same level (Figs. 5–6) as well as from level to level (Fig. 7). In the latter Schwann cell, spiral reversal occurs at four consecutive levels. The three-dimensional contour of this mesaxon is shown in Fig. 8, both in relation to the helical nucleus and as an isolated membrane sheet. In addition to having major variations in their contour, the mesaxons, also had many small projections (Figs. 5–6) that often appeared in the adjacent cytoplasm as membrane-limited profiles. Their shape was determined by their orientation in reference to the plane of section. The mesaxon's termination at the axon surface varied from level to level; differences in the number of spiral turns were associated with these shifts rather than those at the origin.

Transition to Compact Myelin

The Schwann cells surrounding the 13 axons in this group were slightly longer (40–90 μ) with centrally located ellipsoidal nuclei. As the number of spiral turns increased from one to six, there were fewer major variations in the mesaxon's spiral form; no spirals reversed direction along any internode. There were fewer turns paranodally than in the perinuclear region, in which the transition from a loose to a compact lamellar spiral generally occurred (Fig. 9). As in the previous group, the mesaxon origin usually remained in the same quadrant, and changes in the number of turns

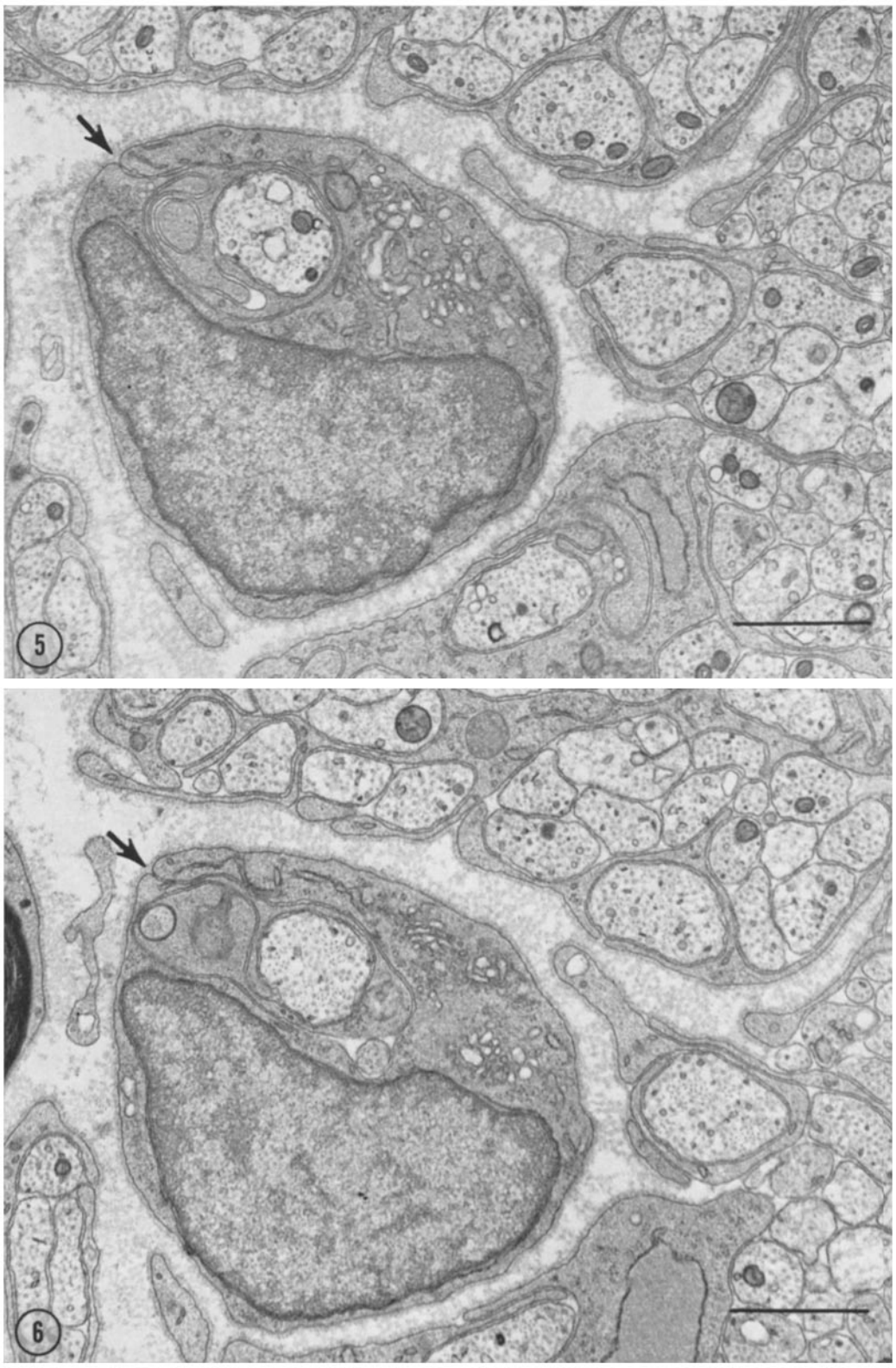

FIGURES 5–6 In two thin sections at the same level, the mesaxon's contour in the nucleated Schwann cell differs. In Fig. 5, after one clockwise turn from its origin (arrow) the mesaxon reverses its direction. A nearby transversely cut projection is sectioned obliquely and is continuous with the mesaxon in Fig. 6. Another small projection is located just above the nucleus in the lower figure. × 21,000.

from level to level were associated with shifts of the mesaxon's termination (7). The diameters for this group's axons were 1.0–1.7 μ. The range was similar for the diameter of the same axon at different levels, and its size was not proportional to that of the myelin spiral. In the four levels of the axon illustrated at the same magnification in Fig. 9, the axon diameter is smaller and the myelin spiral has more turns in Fig. 9 *b* and *c* than in Fig 9 *a* or *d*.

All the compact myelin sheaths in this group had focal regions, usually near the external mesaxon, where the layers were separated by Schwann cell cytoplasm (Figs. 1–4, 7, 9–11). These regions were identified at every level, were almost always located in the same quadrant, and frequently contained organelles. Thus, they appeared to be continuous longitudinal strips that were parallel to the axon and joined the cytoplasm at the Schwann cell's nodal ends. The contour variations in the compact sheaths of this group occurred all along the internode and consisted mainly of redundant loops; some, however, were extremely complex and did not always surround axonal projections (Fig. 10). Also, isolated lamellar bodies, whose periodicity was either similar to myelin or variable, were found most commonly near the external mesaxon in the perinuclear region (Figs. 11, 12). A few growth spirals, similar to those described by Robertson (7), were also observed.

Growth of the Compact Myelin Sheath

Axons in this group measured 1.3–1.9 μ in diameter. Some of the largest myelin sheaths had 17–28 spiral turns and were 70–120 μ long. As the size of the sheath increased, the number of spiral turns was more uniform along the internode. In some Schwann cells, the number of turns at successive levels increased from the paranodal to the perinuclear region. In these myelin spirals, both the mesaxon's origin and termination shifted in directions opposite to each other and appropriate for increasing the number of turns. Generally, the shift at the origin was much greater and accounted for most of the increase in the number of turns at successive levels in the same myelin spiral. Also, major variations in the sheath's contour were less frequent and were located paranodally.

In the Schwann cells containing this group's thinner sheaths (six to ten spiral turns), thin folds, projections, or collars of cytoplasm were occasionally observed along their surface membranes (Fig. 11) or inner mesaxons (Fig. 13). The cytoplasmic strips were not observed at every level and were often displaced tangentially (Figs. 1, 11). A gradual transition from this appearance to that of the Schmidt-Lantermann cleft (5) was observed as the size of the sheath increased.

When the large myelin sheaths (more than 15 turns) in this group were compared to those in the 16-day and adult sciatic nerves, two differences were apparent. At age 7 days, the sheaths were surrounded by a thicker collar of cytoplasm that extended along the entire internode and was filled with granular endoplasmic reticulum, Golgi elements, and mitochondria. Also, the external mesaxons were longer; some formed loops (Fig. 14), and others were separated from the outer myelin layer for variable distances along its circumference. These small variations in the outer mesaxon were less frequently observed in myelin sheaths from older nerves.

DISCUSSION

This morphological study has defined several important geometric parameters of myelination in a small population of rat sciatic nerve fibers. Since the fibers were all unmyelinated at birth, the duration of the process was easy to establish. At appropriate intervals, approximate dimensions for the bundle and its largest fibers were measured and calculated at the same relative level in littermates' nerves. These data show that the myelin membrane's dimensions increased exponentially with time at a much greater rate than the axonal and endoneurial surface membranes of the same Schwann cells (Fig. 15, Table I). Also, dimensions of two groups of smaller fibers in the 7 day nerve (Table II) were in the same range as values for the largest fibers in the 1- and 3-day nerves. The similarity of these data justified the use of three-dimensional reconstructions of cells from the 7 day nerve to describe the intercellular relationships at the onset of myelination and the myelin membrane's shape during its subsequent growth in the bundle's largest fibers.

Myelin formation began in relatively short, ellipsoidal Schwann cells that were arranged in columns and had thin, radially oriented processes that surrounded groups of small, unmyelinated axons. Paranuclear processes of some cells in a column enveloped a single axon at several levels and provided it with small, separate mesaxons. Subsequent mitoses at these sites displaced the axon radially and supplied it with a longitudinal

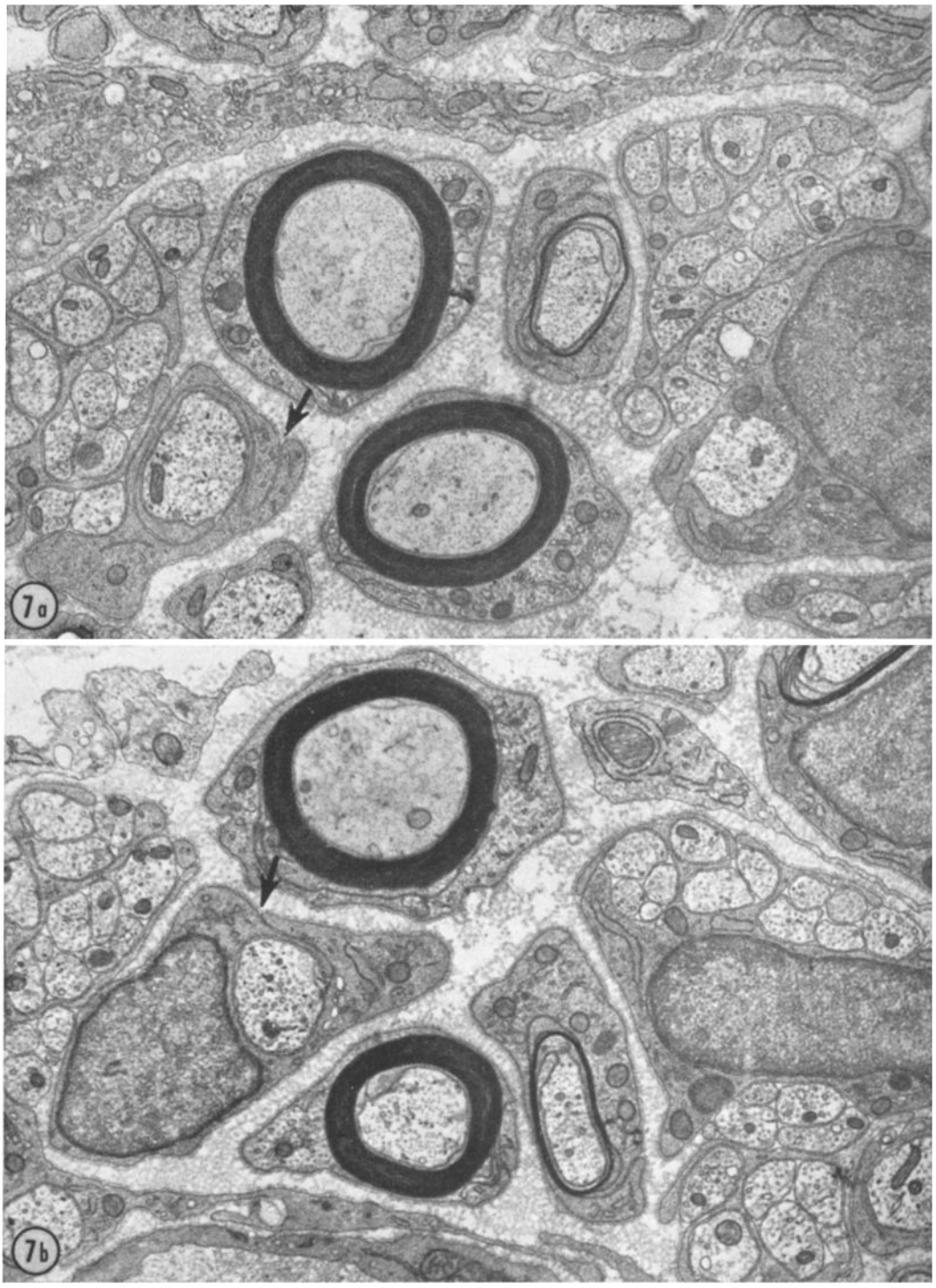

FIGURE 7 The surface relationships of a Schwann cell and its mesaxon contour are shown at four different levels. At the lower left in Fig. 7 *a*, the mesaxon reverses direction a short distance from its origin (arrow) and forms almost one complete anticlockwise turn. To the left, no basal lamina or endoneurial collagen intervenes between the surface membrane, a neighboring Schwann cell, and a small axon. The proximal end of the cell's helical nucleus is present in Fig. 7 *b* and the mesaxon's direction is clockwise. It is anticlockwise and lies above the distal end of the nucleus in Fig. 7 *c* but reverses direction again in Fig. 7 *d*. The three small axons next to the lower left portion of the surface membrane in Fig. 7 *b* indent the Schwann cell's surface in Fig. 7 *c* and lie between it and other small axons to the right in Fig. 7 *d*. × 20,000.

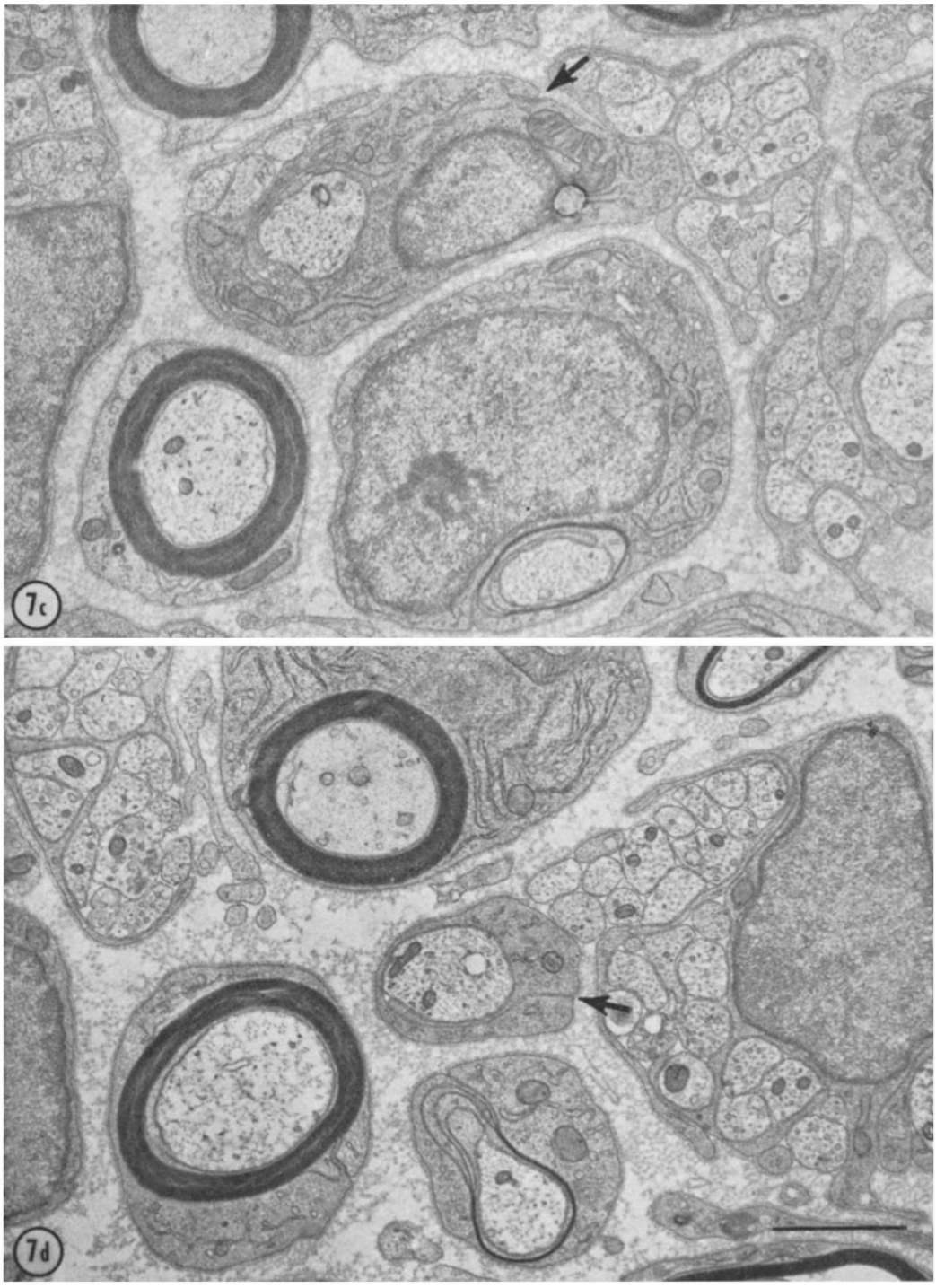
7c
7d

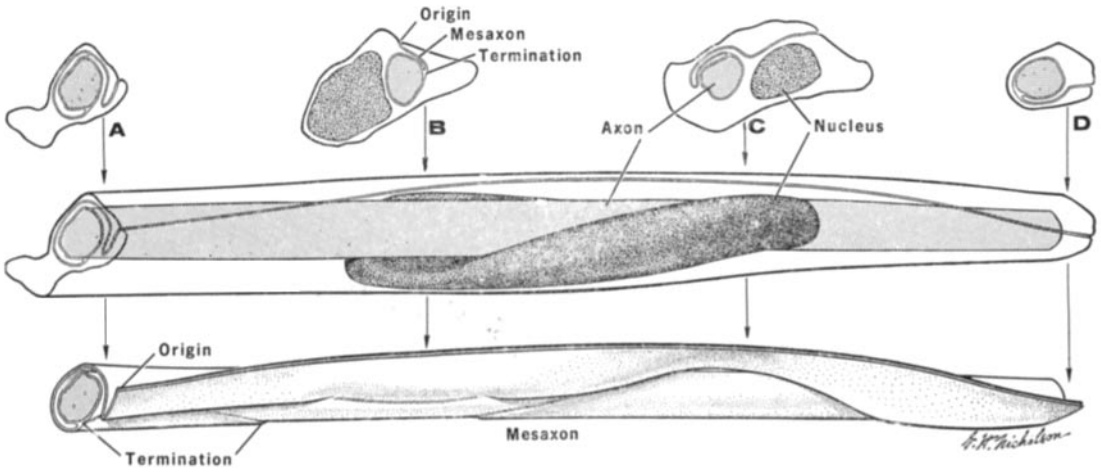

FIGURE 8 Three-dimensional representations of the Schwann cell illustrated in Fig. 7, with the position of the four transverse levels indicated by arrows. The helical nucleus and relatively constant position of the mesaxon's surface origin are included in the upper figure. The lower one shows the mesaxon as a membrane sheet; its contour and transverse length vary.

row of its own satellite cells. (Presumably, this process of segregation, mesaxon formation, and mitosis in the transverse plane progresses distally along the Schwann cell columns and continues at the same level until all the axons destined to be myelinated have been transferred to positions around the periphery of each column.)

While elongating, the daughter Schwann cells acquired a complete basal lamina and then were surrounded by endoneurial collagen. Rapid mesaxon growth began in the paranuclear region and, during the formation of the first spiral turn, there were major level-to-level differences in its size, direction and contour. These differences appeared to be determined by the shape of the nucleus and focal variations in the distribution of organelles. As the number of turns increased, the cytoplasm was gradually confined to a series of continuous longitudinal strips located near the external mesaxon; they contained organelles and probably served as sites for circumferential enlargement and remodelling of the sheath during axonal growth. During this transitional stage, there were fewer differences in the number of turns along the internode, but some variations in the spiral contour persisted. In Schwann cells with compact sheaths consisting of more than six turns, almost all of the cytoplasm was located along the external mesaxon and outer layer of the myelin spiral. Very small ridges were present between the myelin layers at Schmidt-Lantermann clefts and at the nodal ends of the sheath. These tiny helical ridges formed the only connections between the relatively large volume of cytoplasm surrounding the outer layer of the sheath and the rather small collar located along its inner layer. As the elongating Schwann cell's cytoplasm was redistributed in the above manner, the myelin spiral became larger, more circular, and more uniform in contour. As Robertson observed (7), rotation of the mesaxon's axonal end accompanied its growth initially and continued during the subsequent transition from a loose to a compact spiral. Shifts of the mesaxon's origin at the cell surface were usually confined to the nuclear region until the sheath became compact; then, its rotation, in the appropriate direction, accompanied the observed increases in the number of spiral turns. The above changes have been summarized and represented diagrammatically in Fig. 16. In this diagram, the end and face views of the "unrolled" Schwann cells also indicate how much their membrane areas increase during the myelination of a large fiber in this bundle.

Growth rates for compact sheaths surrounding large axons in rat sciatic nerves have already been published (13). Friede and Samorajski have calculated the daily increase in length of a myelin lamella in the sciatic nerves' thickest 10% of fibers from birth to about age 90 days (Fig. 7 in reference 13). At the earliest interval studied, when the

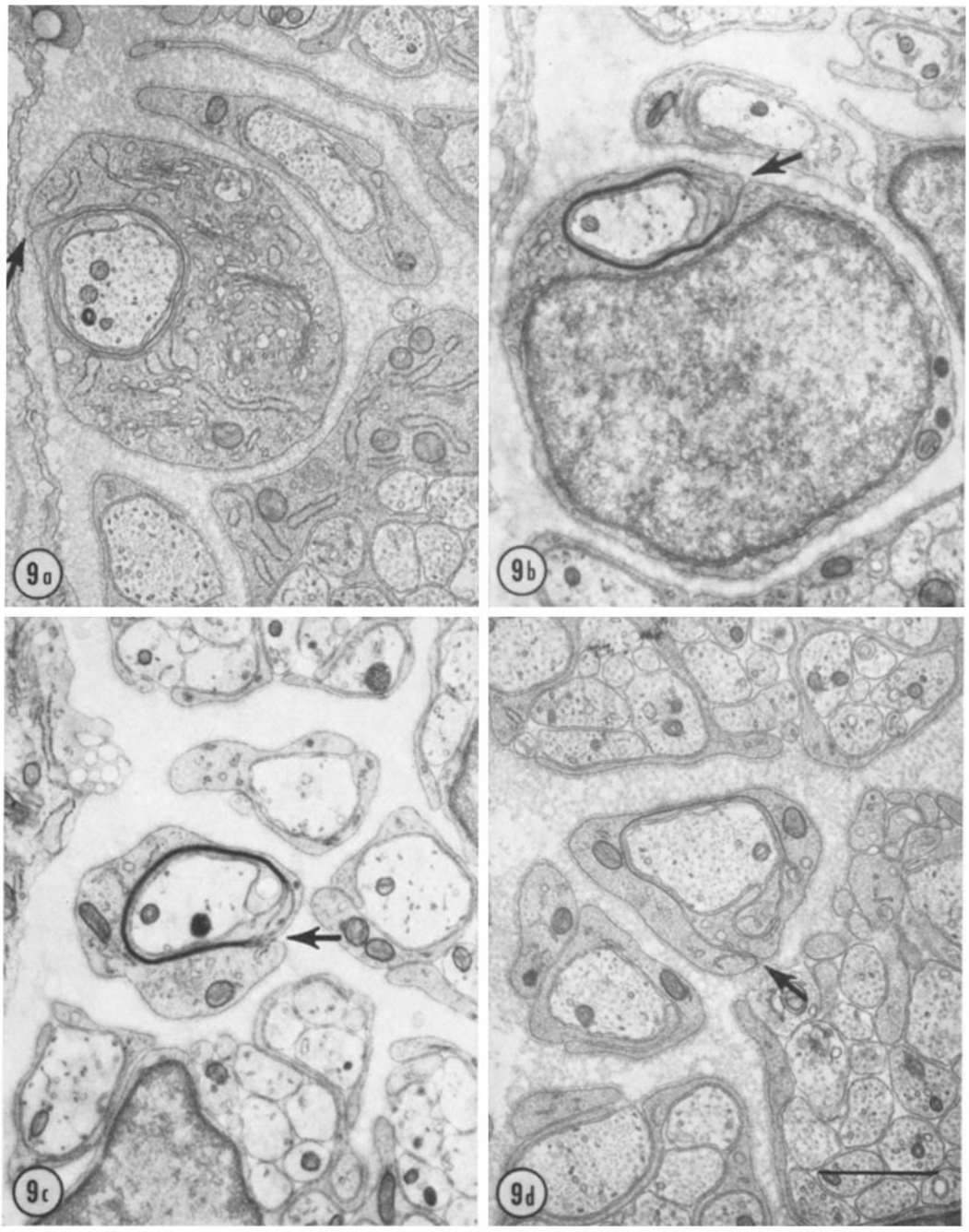

FIGURE 9 Four transverse levels of the same myelinated axons are shown at the same magnification. Proximal to the nucleus in Fig. 9 *a*, there is a loose spiral with 2¼ turns. The myelin sheath has an additional turn in Fig. 9 *b* and *c*; it is compact except near the origin of the external mesaxon (arrows) which shifts 180° from its position in Fig. 9 *a*. More distally (Fig. 9 *d*), the sheath consists of only one spiral turn. × 17,000.

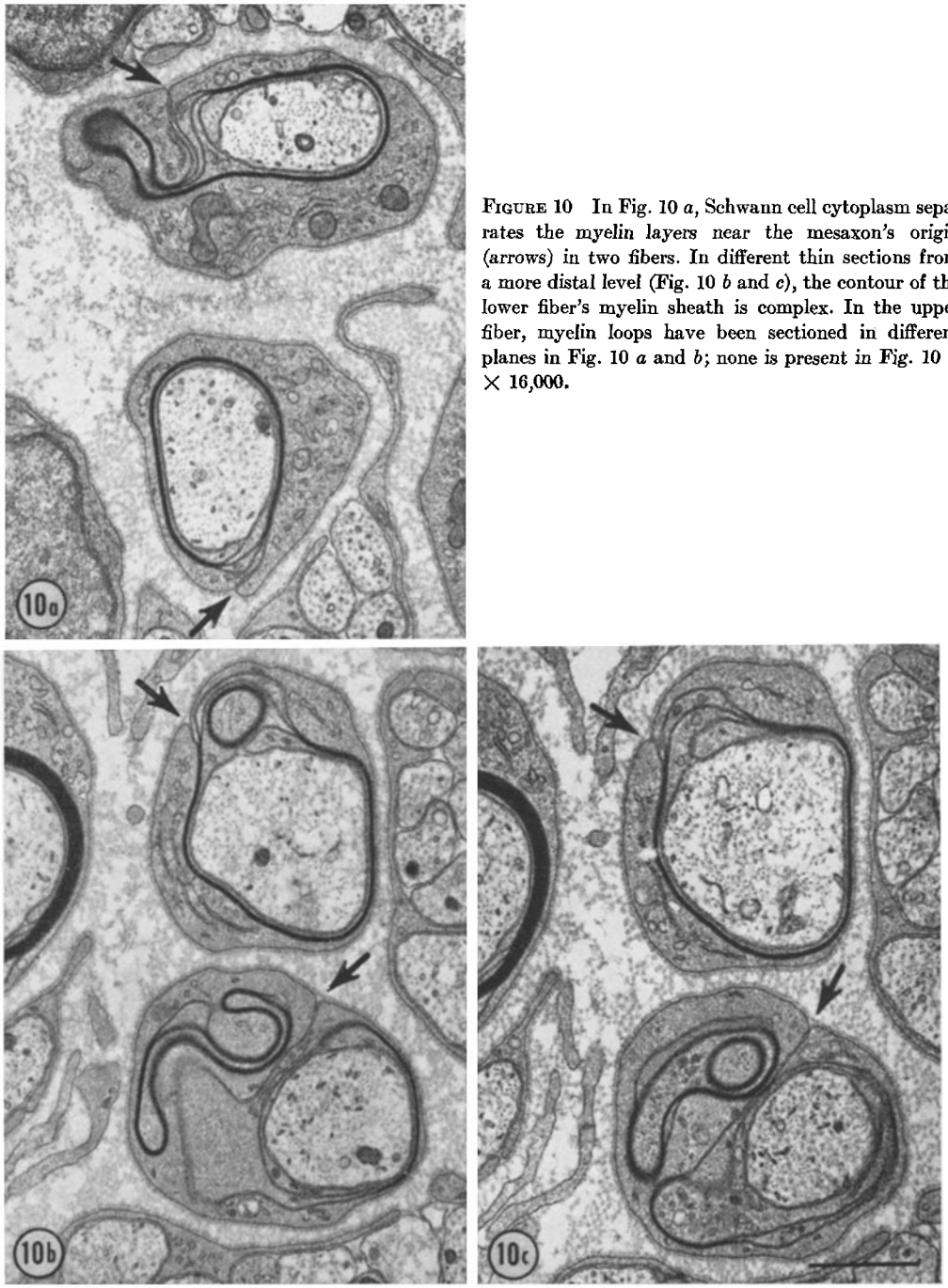

FIGURE 10 In Fig. 10 *a*, Schwann cell cytoplasm separates the myelin layers near the mesaxon's origin (arrows) in two fibers. In different thin sections from a more distal level (Fig. 10 *b* and *c*), the contour of the lower fiber's myelin sheath is complex. In the upper fiber, myelin loops have been sectioned in different planes in Fig. 10 *a* and *b*; none is present in Fig. 10 *c*. × 16,000.

daily increase was lowest, these sheaths already had 6–12 layers (Figs. 6 and 7 in reference 13). The rate then increased more than sixfold to a maximum at age 7–12 days (20–30 layers) and decreased gradually thereafter. In the present study, the rate increased rapidly during growth of the first 4–6 layers and then remained relatively constant during the enlargement of the compact

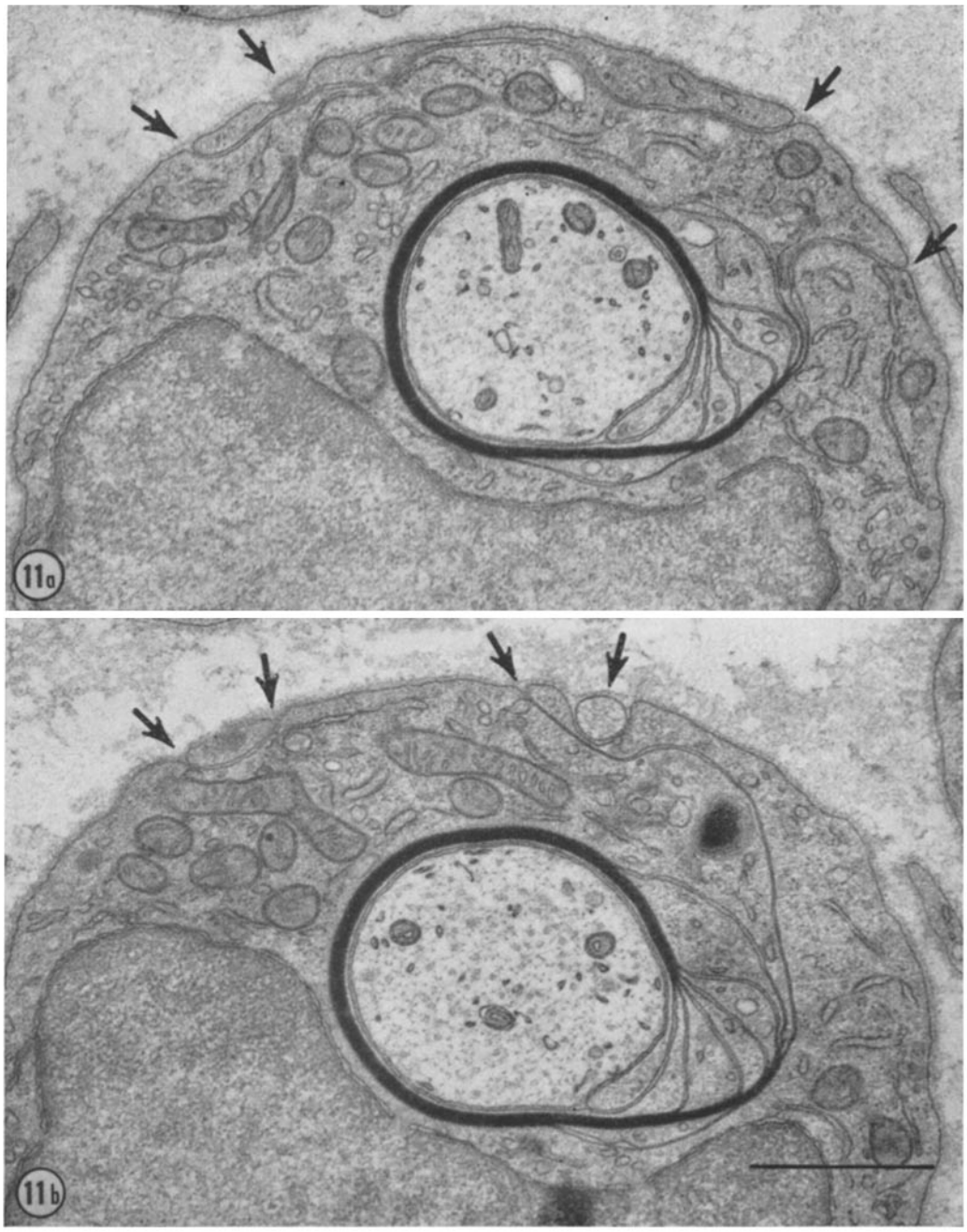

FIGURE 11 The same myelinated fiber is shown in different thin sections at the same level. In Fig. 11 *a*, the mesaxon's origin is to the right (arrow). Above, three arrows indicate a small projection and the ends of a surface strip. The location of the mesaxon's origin differs in Fig. 11 *b* as do the position and size of the projections (arrows). The density and periodicity vary in the lamellar body to the left of the mesaxon. × 26,000.

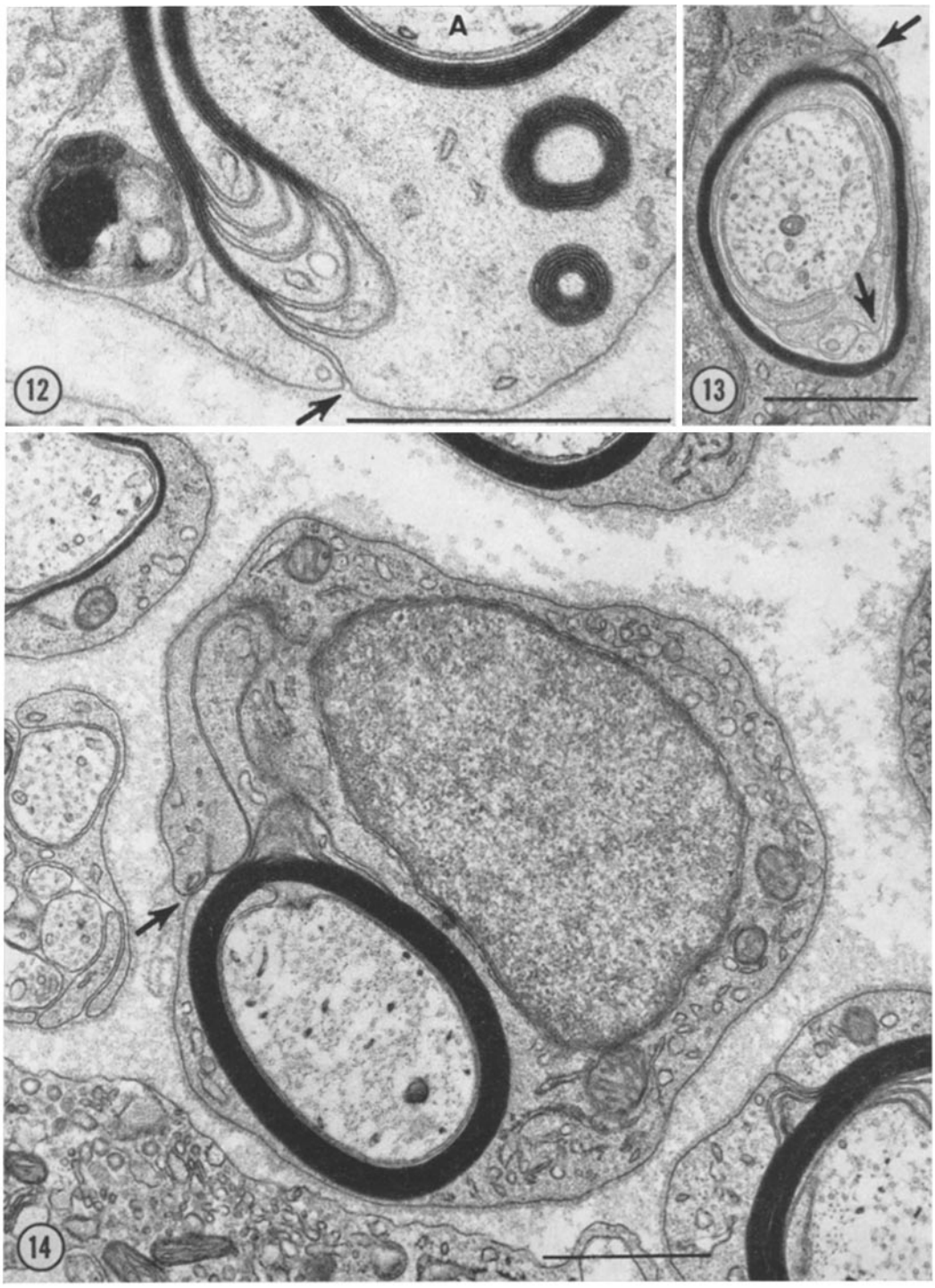

FIGURE 12 Three lamellar bodies are located in the cytoplasm below the axon (*A*). One has amorphous dense areas and an irregular layered structure. The other two have the same periodicity as the adjacent myelin, appear to be isolated in the cytoplasm, and are circular in shape. × 50,000.

FIGURE 13 At the level of this Schwann cell's nucleus, a cytoplasmic collar and projection lie between the mesaxon's termination (lower arrow) and the axon. The myelin sheath is compact except for focal separation of the outer layer near the mesaxon's origin (upper arrow). × 22,000.

FIGURE 14 There is a long loop in the mesaxon between its origin (arrow) and the outer layer of the compact myelin sheath. × 25,000.

spiral. The discrepancies in these quantitative descriptions of myelin membrane growth in rat sciatic nerves probably reflect differences in the stages of myelination studied, the fiber populations, the sampling procedures, the measurements, and the assumptions included in the calculations.

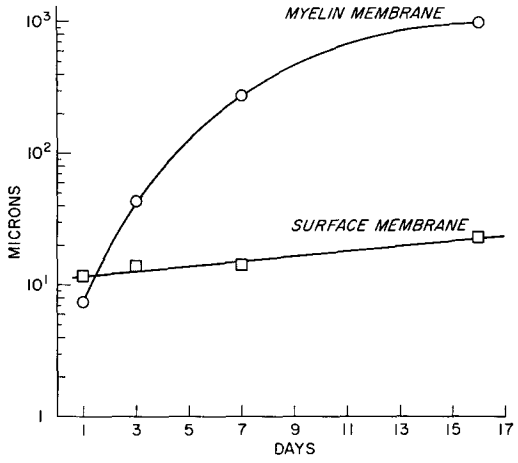

FIGURE 15 Approximate linear dimensions of myelin and surface membranes in transversely sectioned Schwann cells during myelination.

Mechanism of Spiral Formation and Growth

Our observations suggest that the spiral form and initial enlargement of the myelin sheath can be explained, in part, by developmental events which impose mechanical limits on the geometry of the rapid membrane growth that occurs in these Schwann cells. In the cellular columns that surround unmyelinated axons, the arrangement of processes is consistent with a relatively free pattern of surface growth. After mitosis, the daughter cells acquire a basal lamina and become surrounded by endoneurial collagen, both of which probably limit radial spread and favor growth along and around the axon. Surface elongation predominates until proximal and distal Schwann cells meet at the nodes of Ranvier. The sequential establishment of these restrictions helps shift the major site for membrane expansion from the Schwann cell's concentric, cylindrical surfaces to the membrane pair that connects them, the mesaxon. Initially, the position of its outer edge remains relatively fixed while its inner edge remains free to rotate around the axon. These conditions seem consistent geometrically with a situation that would favor spiral formation and

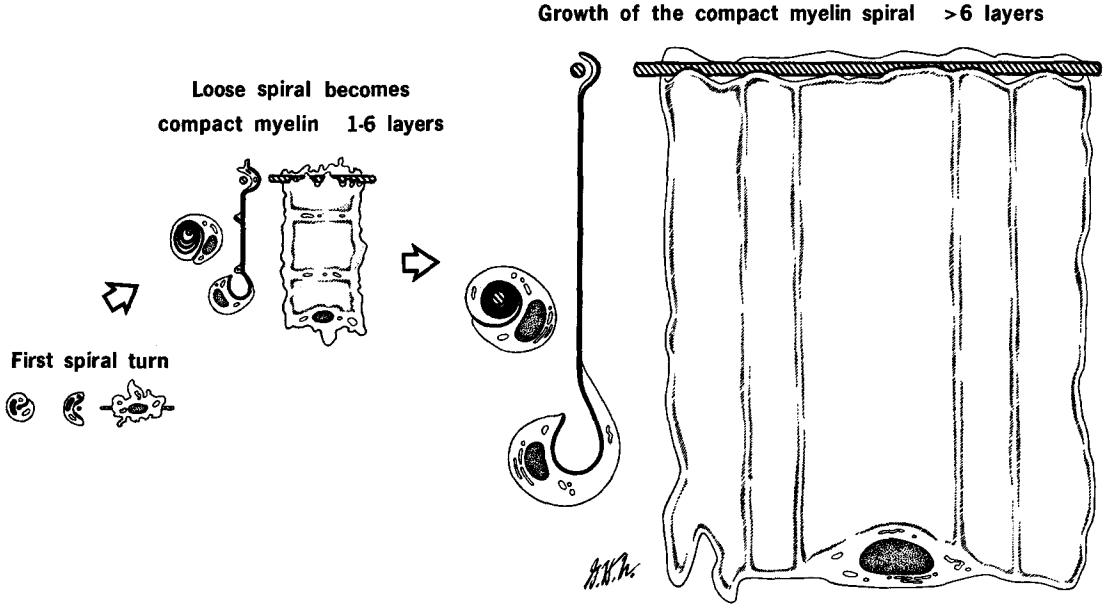

FIGURE 16 A diagram of myelin formation in a Schwann cell that shows how the location and relative size of the myelin membrane's cytoplasmic interfaces change during the sheath's growth. The Schwann cell's appearance in cross-sections is supplemented by transverse and face views of the "unrolled" cell. (To facilitate comparison, the three stages are drawn at the same magnification.)

growth of the mesaxon regardless of where new membrane material were added. Periaxonal rotation of the Schwann cell nucleus (10) may occur, but it does not appear to be an essential prerequisite for spiral formation.

The mesaxon's growth rate increases rapidly. The spiral enlarges, becomes more compact, and the relative area of myelin membrane that is covered by cytoplasm begins to decrease. As these surface relationships change, the rate of membrane growth levels off and its geometry becomes more regular.

The greatest increase in myelin membrane area occurs at a relatively constant rate while the sheath is a compact lamellar spiral. Its length and internal circumference become larger; the number of turns also increases. How this happens remains poorly understood. Our data indicate that the mesaxons, the incisures, and the sheath's outer and inner layers are large enough interfaces for the addition of new membrane material from the cytoplasm at the rate required for the sheath's growth. Membrane components may also gain access to the entire myelin membrane surface more easily than is suggested by its compact lamellar appearance in electron micrographs. Several studies have shown that the intermediate lines in the compact myelin sheath are double (30–32), that extracellular tracers, such as lanthanum, are observed between myelin layers (31), and that labeled amino acids enter the axon after penetrating the Schwann cell and its myelin sheath (33).

As others have suggested (7, 23, 15, 12, 13, 20), the positions of the layers and their components probably change continuously to achieve the best packing arrangement for the molecular constituents of the growing sheath. A dynamic concept for the structural organization of myelin has been included in studies that have demonstrated differences in the composition of myelin during its maturation (34) and in the turnover of some of its ponents (35). As the number of spiral turns increases, the origin of the external mesaxon and the nucleus probably move around the axon. Rotation, in the opposite direction, of the sheath itself and the internal mesaxon may also occur.

This study was begun in the Department of Neurology and the Bascom Palmer Eye Institute at the University of Miami School of Medicine with the support of United States Public Health Service Research Grant No. NB-0711; Dr. Frank Bishop spent a student elective working on this project.

Miss Maureen O'Connell's help in preparing the material and making many of the measurements was greatly appreciated. The suggestions of Drs. Ernst Freese and Milton Brightman were useful in revising the manuscript.

Received for publication 5 June 1970, and in revised form 30 July 1970.

REFERENCES

1. GEREN, B. B. 1954. The formation from the Schwann cell surface of myelin in the peripheral nerves of chick embryos. *Exp. Cell Res.* 7:558.
2. ROBERTSON, J. D. 1955. The ultrastructure of adult vertebrate peripheral myelinated nerve fibers in relation to myelinogenesis. *J. Biophys. Biochem. Cytol.* 1:271.
3. GEREN, B. B. 1956. Structural studies of the formation of the myelin sheath in peripheral nerve fibers. *In* Cellular Mechanisms in Differentiation and Growth. D. Rudnick, editor. Princeton University Press, Princeton, N. J. 213.
4. ROBERTSON, J. D. 1957. New observations on the ultrastructure of the membranes of frog peripheral nerve fibers. *J. Biophys. Biochem. Cytol.* 3:1043.
5. ROBERTSON, J. D. 1958. The ultrastructure of Schmidt-Lantermann clefts and related shearing defects of the myelin sheath. *J. Biophys. Biochem. Cytol.* 4:39.
6. PETERS, A., and A. R. MUIR. 1958. The relationship between axons and Schwann cells during development of peripheral nerves in the rat. *J. Exp. Physiol.* 44:117.
7. ROBERTSON, J. D. 1962. The unit membrane of cells and mechanisms of myelin formation. *Res. Publ. Ass. Res. Nerv. Ment. Dis.* 40:94.
8. SJOSTRAND, F. S. 1963. The structure and formation of the myelin sheath. *In* Mechanisms of Demyelination. A. S. Rose and C. M. Pearson, editors. McGraw Hill Publishing Co., New York. 1.
9. ROBERTSON, J. D. 1964. Unit membranes: A review with recent new studies of experimental alterations and a new subunit structure in synaptic membranes. *In* Cellular Membranes in Development. M. Locke, editor. Academic Press Inc., New York. 1.
10. MURRAY, M. R. 1965. Nervous tissues *in vitro*. *In* Cells and Tissues in Culture. E. N. Willmer editor. Academic Press Inc., New York 2:373.
11. FRIEDE, R. L., and T. SAMORAJSKI. 1967. Relation between the number of myelin lamellae and

axon circumference in fibers of vagus and sciatic nerves of mice. *J. Comp. Neurol.* **130**:223.

12. BUNGE, R. P. 1968. Glial cells and the central myelin sheath. *Physiol. Rev.* **48**:197.
13. FRIEDE, R. L., and T. SAMORAJSKI. 1968. Myelin formation in the sciatic nerve of the rat. A quantitative electron microscopic, histochemical and radioautographic study. *J. Neuropathol. Exp. Neurol.* **27**:546.
14. MATTHEWS, M. A. 1968. An electron microscopic study of the relationship between axon diameter and the initiation of myelin production in the peripheral nervous system. *Anat. Rec.* **161**:337.
15. UZMAN, B. G., and E. T. HEDLEY-WHYTE. 1968. Myelin: dynamic or stable? *J. Gen. Physiol.* **51**: 85.
16. ALLT, G. 1969. Ultrastructural features of the immature peripheral nerve. *J. Anat.* **105**:283.
17. FRIEDE, R. L., and T. SAMORAJSKI. 1969. The clefts of Schmidt-Lantermann: A quantitative electron microscopic study of their structure in developing and adult sciatic nerves of the rat. *Anat. Rec.* **165**:89.
18. HEDLEY-WHYTE, E. T., F. A. RAWLINS, M. M. SALPETER, and B. G. UZMAN. 1969. Distribution of cholesterol-I, 2-H^3 during maturation of mouse peripheral nerve. *Lab. Invest.* **21**:536.
19. HENDELMAN, W. J., and R. P. BUNGE. 1969. Radioautographic studies of choline incorporation into peripheral nerve myelin. *J. Cell Biol.* **40**:190.
20. PETERS, A., S. L. PALAY, and H. DEF. WEBSTER. 1970. The Fine Structure of The Nervous System. The Cells and Their Processes. Harper & Row, New York.
21. WEBSTER, H. DEF., and D. SPIRO. 1960. Phase and electron microscopic studies of experimental demyelination. I. Variations in myelin sheath contour in normal guinea pig sciatic nerve. *J. Neuropathol. Exp. Neurol.* **19**:42.
22. WEBSTER, H. DEF. 1964. Some ultrastructural features of segmental demyelination and myelin regeneration in peripheral nerve. *In* Progress in Brain Research. Mechanisms of Neural Regeneration. M. Singer and J. P. Schade, editors. Elsevier Publishing Co., New York. **13**:151.
23. ROSENBLUTH, J. 1966. Redundant myelin sheaths and other ultrastructural features of the toad cerebellum. *J. Cell Biol.* **28**:73.
24. HAYAT, M. A. 1968. Triple fixation for electron microscopy. *In* Proceedings, Twenty-sixth Annual Meeting Electron Microscopy Society of America. C. J. Arceneaut, editor. Claitor's Publishing Division, Baton Rouge, La. 90.
25. WEBSTER, H. DEF. 1969. The pattern of membrane growth in Schwann cells during the formation and enlargement of peripheral myelin sheaths. *J. Cell Biol.* **43**:154 a. (Abstr.)
26. LUFT, J. H. 1961. Improvements in epoxy embedding methods. *J. Biophys. Biochem. Cytol.* **9**:409.
27. STEINBRECHT, R. A., and K. D. ERNST. 1967. Continuous penetration of delicate tissue specimens with embedding resin. *Sci. Tools.* **14**:24.
28. ROCKWELL, A., P. NORTON, J. B. CAULFIELD, and S. ROTH. 1966. A silicone rubber mold for embedding tissue in epoxy resins. *Sci. Tools.* **13**:9.
29. VENABLE, J., and R. COGGESHALL. 1965. A simplified lead citrate stain for use in electron microscopy. *J. Cell Biol.* **25**:407.
30. ROBERTSON, J. D. 1961. Cell membranes and the origin of mitochondria. *In* Regional Neurochemistry. S. S. Kety, editor. Pergamon Press, New York. 497.
31. REVEL, J. P., and D. W. HAMILTON. 1969. The double nature of the intermediate dense line in peripheral nerve myelin. *Anat. Rec.* **163**:7.
32. NAPOLITANO, L. M., and T. J. SCALLEN. 1969. Observations on the fine structure of peripheral nerve myelin. *Anat. Rec.* **163**:1.
33. CASTON, J. D., and M. SINGER. 1969. Amino acid uptake and incorporation into macromolecules of peripheral nerves. *J. Neurochem.* **16**:1309.
34. HORROCKS, L. A. 1968. Composition of mouse brain myelin during development. *J. Neurochem.* **15**:483.
35. SMITH, M. E. 1968. The turnover of myelin in the adult rat. *Biochem. Biophys. Acta.* **164**:285.